66, 373 (1991).
3. P. D. Zamore and M. R. Green, *Proc. Natl. Acad. Sci. U.S.A.* **86**, 9243 (1989); *EMBO J.* **10**, 207 (1991).
4. X.-D. Fu and T. Maniatis, *Nature* **343**, 437 (1990); D. L. Spector *et al.*, *EMBO J.* **10**, 3467 (1991).
5. X.-D. Fu and T. Maniatis, *Proc. Natl. Acad. Sci. U.S.A.* **89**, 1725 (1992).
6. Purification of SC35. HeLa nuclear extract (10 ml) was mixed with an equal volume of saturated ammonium sulfate (AS), and the mixture was stirred at 4°C for 1 hour. The precipitate was removed by centrifugation at 4000 rpm ($4657g_{max}$) for 30 min. in a Beckman centrifuge H-6000A. When assayed by immunoblotting, SC35 was found in the soluble fraction. The SC35-containing fraction was applied to a 3-ml (packed volume) phenyl-Sepharose (Pharmacia) column equilibrated in buffer A (20 mM tris-HCl, pH 7.9; 100 mM KCl; 0.2 mM EDTA) plus 1.7 M AS. After washing the column with 5 ml of the same buffer, proteins were step-eluted with buffer A plus 0.2 M incremental decreases in AS concentration or with buffer A alone. SC35 was eluted in two peaks at 1.3 M and 0.5 M AS. The 1.5 to 1.1 M fractions containing SC35 were combined, dialyzed overnight against buffer B (buffer A plus 5% glycerol), concentrated on a Centriprep 30 (Amicon), and loaded onto a MonoQ column (Pharmacia) equilibrated in the same buffer. The MonoQ column was developed with a linear KCl concentration gradient from 0.1 to 1.0 M KCl in buffer B, and 1-ml fractions were collected. SC35 was eluted in one peak at 0.35 M KCl, and the pooled MonoQ fractions were used for peptide sequencing analysis in this study. The peak fraction was further fractionated on a glycerol gradient, concentrated on a Centricon 30, and loaded onto a 10 to 30% linear glycerol gradient, followed by centrifugation at 47,000 rpm for 23 hours at 4°C in a Beckman SW55 rotor. After centrifugation, 0.5-ml fractions were collected. SC35 was apparently homogeneous in one of the fractions and was used for protein composition determination or for functional analyses.
7. Isolation of SC35 cDNA clones. Two DNA oligomers (probe A and probe B) were synthesized according to the sequence of peptide 1 (Fig. 1). These two probes were end-labeled with [^{32}P]ATP and T4 kinase. The labeled probes were used to screen 0.5 × 10^6 plaques from a human B cell primary cDNA library with the TMACl (tetramethylammonium chloride) hybridization protocol (*8*). The SC35 insert was isolated from phage DNA, subcloned into the Eco RI site of the pSP73 vector (pSP73-SC35), and sequenced.
8. J. Sambrook, E. Fritsch, T. Maniatis, *Molecular Cloning: A Laboratory Manual* (Cold Spring Harbor Laboratory, Cold Spring Harbor, NY, ed. 2, 1989).
9. M. Kozak, *Cell* **44**, 283 (1986).
10. The open reading frame of p1B cDNA contains 24% arginine and 20% serine residues, compared to 27% arginine and 18% serine of purified SC35. The calculated isoelectric point for the protein encoded by the clone is 12.38.
11. H. Amrein, *Cell* **55**, 1025 (1989); T. J. Goralski *et al.*, *ibid.* **56**, 1011 (1989).
12. A. Mayeda, A. M. Zahler, A. R. Krainer, M. B. Roth, *Proc. Natl. Acad. Sci. U.S.A.* **89**, 1301 (1992); A. Zahler, W. Lane, M. Roth, *Genes Dev.*, in press.
13. X.-D. Fu and T. Maniatis, unpublished data.
14. M. D. Summers and G. E. Smith, *A Manual of Methods for Baculovirus Vectors and Insect Cell Culture Procedures*, Texas Agricultural Experiment Station, Bulletin no. 1555 (1987). An Eco RV–Pvu II fragment that contained SC35 from pSP73-SC35 was cloned into the Nhe I site of the baculovirus expression vector pJVP10Z. The translation initiation signal of SC35 was used in this construct. Recombinant virus expressing SC35 was produced according to the manual. Insect cell nuclear extracts containing SC35 or bicoid were prepared in the same way as HeLa nuclear extracts, and 5 ml of nuclear extract were obtained from 100 ml of infected sf9 cells (1 × 10^8). Depletion and complementation analyses were as described (*4, 5*) and modified (*5*).
15. G. Dreyfus *et al.*, *Trends Biochem. Sci.* **13**, 86 (1988); D. J. Kenan *et al. ibid.* **16**, 214 (1991); C. C. Query *et al.*, *Cell* **57**, 89 (1989).
16. H. Li and P. M. Bingham, *Cell* **67**, 335 (1991).
17. M. B. Roth *et al.*, *J. Cell Biol.* **111**, 2217 (1990); *ibid.* **115**, 587 (1991).
18. D. Rosson and E. P. Reddy, *Nature* **319**, 604 (1986).
19. M. Vellard *et al.*, *Oncogene* **6**, 505 (1991).
20. B. Perbal and M. Vellard, *C. R. Acad. Sci. Paris* **311**, 467 (1990); M. Vellard *et al.*, *ibid.* **313**, 591 (1991).
21. A. Sureau and B. Perbal, *ibid.* **312**, 323 (1991).
22. We thank A. Krainer, J. Manley, H. Ge, and M. Roth for communicating their unpublished results; W. Lane for amino acid composition and peptide sequencing; X.-F. Wang, H. Wu, and M.-J. Jin for advice on Northern blotting analyses and peptide tagging; A. Leza for computer sequence homology search; G. Shen-Ong for many insights into the c-*myb* proto-oncogene; R. Kriz for the human B cell primary cDNA library; K. Diepold for the recombinant virus–expressing bicoid; and J. Bruzik, J. Wu, M. Tian, H. Amrein, M-L. Hedley, T. Schaal, and members of the Maniatis laboratory for useful discussions and critical comments on the manuscript. Supported by NIH grant GM42231 to T.M.

15 January 1992; accepted 6 March 1992

Regulatory Elements That Control the Lineage-Specific Expression of *myo*D

David J. Goldhamer, Alexander Faerman, Moshe Shani, Charles P. Emerson, Jr.*

The molecular basis of skeletal muscle lineage determination was investigated by analyzing DNA control elements that regulate the myogenic determination gene *myo*D. A distal enhancer was identified that positively regulates expression of the human *myo*D gene. The *myo*D enhancer and promoter were active in myogenic and several nonmyogenic cell lines. In transgenic mouse embryos, however, the *myo*D enhancer and promoter together directed expression of a *lac*Z transgene specifically to the skeletal muscle lineage. These data suggest that during development *myo*D is regulated by mechanisms that restrict accessibility of *myo*D control elements to positive trans-acting factors.

The formation of differentiated tissue types during development involves the determination of specific cell lineages from multipotential progenitor cells followed by terminal differentiation, resulting in cell type–specific gene expression and function. The molecular mechanisms that regulate cell lineage determination are poorly understood. However, the mouse cell line C3H10T1/2 (10T1/2) has provided a model cell culture system (*1*) that has allowed identification of four mammalian genes [*myo*D (*2*), *myogenin* (*3*), *Myf*-5 (*4*), and *MRF*-4 (*5*)] that regulate the determination of the skeletal muscle lineage (*6*). These genes encode transcription factors that comprise a subgroup within the helix-loop-helix (HLH) superfamily of Myc-related DNA binding proteins (*7*). As transfected complementary DNAs (cDNAs), these factors induce myogenic conversion of multipotential 10T1/2 cells to stably determined populations of proliferative myogenic cells (*2–5*). Consistent with a function in determination, these myogenic regulatory genes are expressed exclusively in skeletal muscle lineages of the embryo, beginning at early stages of somite formation (*8–10*). Although the function of the proteins encoded by these genes is beginning to be elucidated (*6*), the transcriptional regulatory mechanisms that activate their expression in the skeletal muscle lineage of the embryo are unknown.

We have analyzed the cis-acting DNA sequences that regulate expression of the human *myo*D gene. A pWE15 cosmid library was screened at moderate stringency with a full-length mouse MyoD cDNA (*11*). This screen yielded four recombinants representing three unique overlapping clones that spanned a total of 40 kb. Sequence comparison with the human MyoD cDNA (*12*) identified the hybridizing species as *myo*D. The organization of the cosmid clone used in subsequent analyses (chMD-*13*) included ~25.5 kb of DNA upstream and 4 kb downstream of the *myo*D gene (Fig. 1A).

Transcriptional activity of the *myo*D promoter was assayed in 23A2 myoblasts, myogenic cells derived from the multipotential 10T1/2 cell line by 5-azacytidine treatment (*1*). We fused 2.5 kb of 5′ flanking sequence of *myo*D to the chloramphenicol acetyltransferase (CAT) reporter gene (−2.5CAT; Fig. 1A) (*13*), and CAT activity was assayed after transient transfection into proliferative 23A2 myoblasts (*14*). The *myo*D promoter is only weakly

D. J. Goldhamer and C. P. Emerson, Jr., Institute for Cancer Research, Fox Chase Cancer Center, Philadelphia, PA 19111.
A. Faerman and M. Shani, Institute of Animal Science, Volcani Center, P.O. Box 6, Bet Dagan, 50250 Israel.
*To whom correspondence should be addressed.

active in 23A2 myoblasts, yielding CAT activity five- to tenfold greater than a promoterless CAT construct (PoCAT; Fig. 1B) and ~20% of the activity of the herpesvirus thymidine kinase (HSVtk) promoter (*15*).

The discrepancy between the low activity of the transfected *myo*D promoter and high expression of the endogenous *myo*D gene in 23A2 cells (*16*) suggested that sequences outside of the proximal 2.5 kb of 5′ flanking sequence regulate *myo*D expression. Therefore, 24 kb of contiguous 5′ sequence was tested for activity by transient transfection (Fig. 1, A and B). CAT activity was increased ~ tenfold above that of the promoter alone when these upstream sequences were included (Fig. 1B). To localize the positive regulatory element or elements, we cloned a series of nonoverlapping restriction fragments that span the 24-kb upstream sequence into −2.5CAT, and we tested for their ability to enhance transcription from the promoter in 23A2 myoblasts. This enhancing activity (Fig. 1B) was quantitatively recovered in a fragment 18 to 22 kb 5′ to *myo*D (fragment 3) (Fig. 1A).

A clone that contains the 24 kb of 5′ flanking sequence except for fragment 3 (−24ΔF3CAT), exhibited CAT activity comparable to the promoter-containing fragment alone (Fig. 1B) (*17*). These results demonstrate that fragment 3 contains the only positive sequence elements within the 24 kb that significantly enhanced activity of the *myo*D promoter. Similar results were obtained in transient transfection assays of C2C12 myogenic cells (*15*).

We next showed that fragment 3 contains one or more enhancers by demonstrating that it enhanced activity of the HSVtk promoter and was equally effective in both orientations (Fig. 2). In addition, fragment 3 in either orientation exhibited only background CAT activity in a promoterless CAT construct (*15*), demonstrating that fragment 3 does not contain promoter activity.

Because *myo*D is expressed exclusively in skeletal muscle, we investigated the muscle-specificity of the distal enhancer and promoter. The 10T1/2 cells are nonmyogenic and do not express *myo*D, but are converted to myogenic cells by 5-azacytidine (*1*), by forced expression of the myogenic regulatory cDNAs (*2–5*), and by transfection of the genomic locus *myd* (*18*). The *myo*D promoter and enhancer, as well as the entire 24 kb of 5′ flanking sequence, were as active in 10T1/2 cells as in 23A2 myoblasts (Fig. 3). In stable transfection assays, these control elements also showed comparable activity in 10T1/2 and 23A2 cells (*15*). In contrast, the transfected myogenin promoter is inactive in 10T1/2 cells (*19*), suggesting that the transcriptional control of these two myogenic regulatory genes is fundamentally different. Subsequently, we tested a variety of cell lines to determine whether multipotential 10T1/2 cells were unique among nonmyogenic cells in their ability to express the *myo*D promoter and enhancer. These include Ltk$^-$ cells, three 10T1/2-derived adipocyte cell lines, BNL liver cells, HepG2 hepatoma cells, and JEG-3 choriocarcinoma cells. The *myo*D enhancer and promoter were active in all of these cell lines except JEG-3 cells (Fig. 3) (*15*). Activity was relatively low in HepG2 cells (Fig. 3) but in the other cell lines was comparable to that in 23A2 myoblasts. Similarly, the resident human *myo*D gene was activated when chromosome 11 was transferred from primary hu-

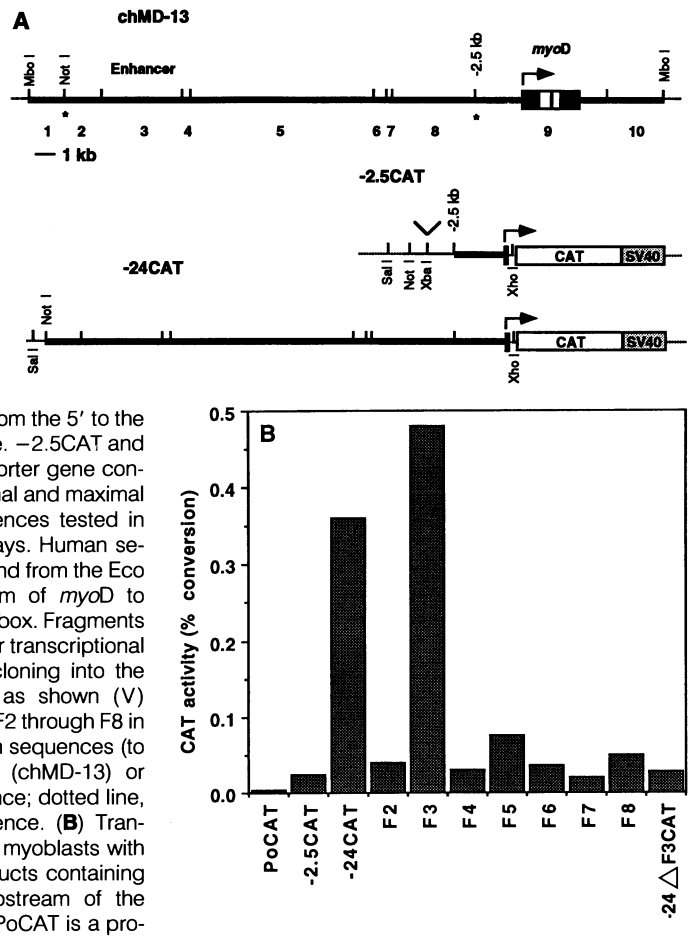

Fig. 1. A distal regulatory element enhances transcriptional activity of the *myo*D promoter. (**A**) Map of human cosmid clone chMD-13. Eco RI (unmarked vertical lines) and Not I restriction sites, and presumed Mbo I cloning sites are indicated. Exons and introns in *myo*D are shown by solid and open blocks, respectively. For reference, restriction fragments for enzymes shown are labeled sequentially from the 5′ to the 3′ end of the cosmid clone. −2.5CAT and −24CAT refer to CAT reporter gene constructs (*13*) with the minimal and maximal amounts of human sequences tested in transient transfection assays. Human sequences in −2.5CAT extend from the Eco RI site ~2.5 kb upstream of *myo*D to +198 relative to the TATA box. Fragments 2 through 8 were tested for transcriptional enhancing activity after cloning into the Xba I site of −2.5CAT, as shown (V) (constructs referred to as F2 through F8 in Fig. 1B). Thick line, human sequences (to scale); thin line, pWE15 (chMD-13) or pBluescript vector sequence; dotted line, ptkCATΔEH vector sequence. (**B**) Transient transfection of 23A2 myoblasts with CAT reporter gene constructs containing 5′ flanking sequence upstream of the human *myo*D gene (*14*). PoCAT is a promoterless CAT gene construct, and −24ΔF3CAT is identical to −24CAT except that fragment 3 is deleted. In all experiments, 0.8 pmol (between 2.1 and 15 μg) of each construct was used per transfection. CAT activity is the percent conversion of ^{3}H-chloramphenicol to butyryl-^{3}H-chloramphenicol per microgram of protein per hour at 37°C. These data are the averages of two independent, representative experiments.

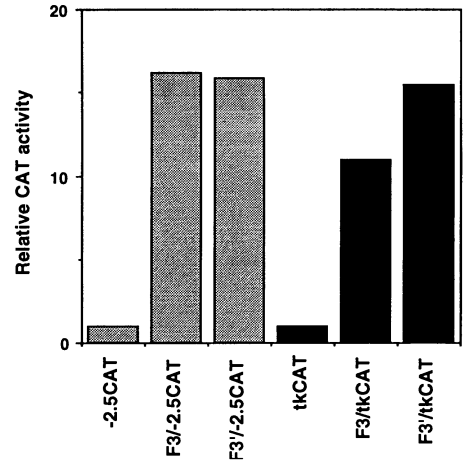

Fig. 2. The *myo*D distal regulatory element contains an enhancer. Fragment 3 was cloned in both orientations in −2.5CAT (F3/−2.5CAT and F3′/−2.5CAT are sense and antisense enhancer orientations, respectively) or upstream of the HSVtk promoter in ptkCATΔEH (F3/tkCAT and F3′/tkCAT), and constructs were tested for activity by transient transfection into 23A2 myoblasts. Data are the averages of at least three independent experiments. CAT activity is presented as relative values compared to activities of −2.5CAT and tkCAT, which were arbitrarily set to a value of 1. Actual percent conversion per microgram of protein: −2.5CAT, 0.03; tkCAT, 0.13.

man fibroblasts to various tissue culture cell lines (*20*). Expression of the *myo*D enhancer and promoter in these nonmyogenic cells, which do not express any known HLH myogenic regulatory proteins, indicates that their activity is not dependent on auto- or cross-activation (*12, 21*) by members of the HLH myogenic protein family.

To determine if the enhancer and promoter confer muscle specificity in vivo, we tested two *lac*Z reporter gene constructs in transgenic mouse embryos (*22*). The promoter/*lac*Z construct (−2.5lacZ) contained 2.5 kb of human sequences 5′ to the *myo*D gene cloned upstream of *lac*Z, whereas the other (F3′/−2.5lacZ) contained the 2.5 kb of flanking DNA as well as the upstream enhancer fragment cloned in an antisense orientation. The −2.5lacZ construct was introduced into nine embryos by pronucleus injection. Whole mount and serially sectioned embryos were analyzed for β-galactosidase (β-gal) activity at 11.5 days postcoitum (p.c.), the time at which myogenic cells of the somitic myotome and limb buds first express *myo*D transcripts at high concentrations (*8, 9*). None of the mouse embryos injected with −2.5lacZ showed *lac*Z expression in somites, limb buds, or any other populations of myogenic cells (Fig. 4A). However, three embryos showed ectopic patterns of β-gal activity (Fig. 4A), but with no consistent pattern of expression. The *lac*Z expression in these ectopic sites is likely a result of integration of the transgene into or next to developmentally expressed genes (*23*).

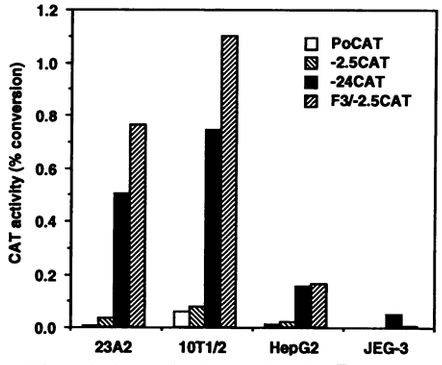

Fig. 3. Cell specificity of the *myo*D promoter and enhancer in myogenic and nonmyogenic cell types. As a positive control for transfections, parallel dishes were transfected with 0.1 μg of an RSVCAT construct. The average percent conversion per microgram protein for each cell type with RSVCAT was: 23A2, 0.6%; 10T1/2, 1.3%; HepG2, 2.3%; JEG-3, 2.8%. We estimated transfection efficiencies by histochemically staining parallel dishes after transfection with a β-actin promoter-driven *lac*Z reporter gene. Average transfection efficiencies for each cell type were: 23A2, 12%; 10T1/2, 17%; HepG2, 8%; JEG-3, 14%. Values shown are not corrected for differences in transfection efficiencies. Data presented are the averages of at least three independent experiments. The lack of enhancer activity in JEG-3 cells was confirmed with the HSVtk promoter (CAT activities of 0.08% and 0.12% conversion per microgram of protein were obtained for tkCAT and F3/tkCAT, respectively).

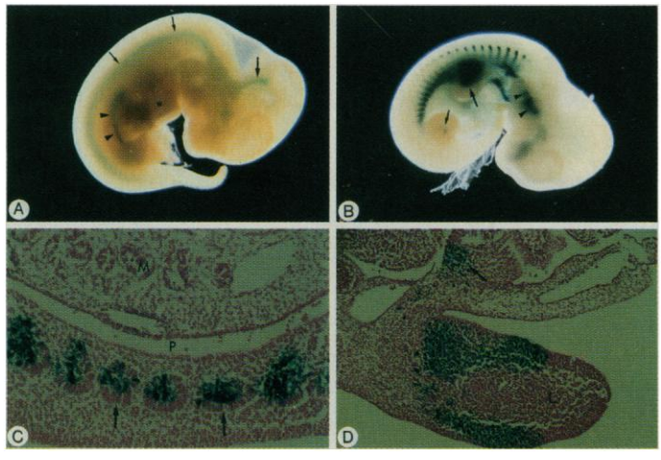

Fig. 4. Embryonic expression of *myo*D *lac*Z transgenes. Embryos were injected with the *myo*D promoter/*lac*Z transgene (−2.5lacZ; panel A) and the *myo*D enhancer/promoter *lac*Z transgene (F3′/−2.5lacZ; panels B, C, and D), and stained for β-gal activity at 11.5 day p.c. (35 to 37 somites). (**A**) Whole mount of a representative transgenic embryo showing ectopic expression of −2.5lacZ. No staining of the somites, limb buds (fore limb bud designated with asterisk) or visceral arches was detected. This embryo shows ectopic staining in the spinal cord (small arrows), mesencephalon (large arrow), and mesonephros (arrowheads). (**B**) Whole mount of a representative transgenic embryo showing expression of the F3′/−2.5lacZ transgene. The *lac*Z expression in the somites is evident as a metameric pattern of staining along the rostro-caudal axis of the embryo. The *lac*Z expression is not evident in somites posterior to the level of the hind-limb bud. The proximal region of the fore-limb bud contains a large population of intensely stained cells (large arrow), whereas few *lac*Z-positive cells are present in the hind limb (small arrow). Intense staining is also observed in the mesoderm of the visceral arches (arrowheads). Weak staining in the head is probably associated with the developing extraocular muscles and nasal pits. (**C**) Frontal section through the somites (approximately somites 10 to 15) of the same transgenic embryo shown in (B). The *lac*Z-expressing cells are restricted to the myotomal compartment of these anterior somites, which at 11.5 days p.c. are differentiating into blocks of myotomal muscle. This section cuts through the ventral lateral portion of the somites, revealing the dermotomes (two designated with arrows) and myotomes (*lac*Z-positive cells) of the somites. P, peritonium; M, mesonephric tubules. (**D**) Frontal section at the level of the forelimb bud of the same embryo shown in (B). The β-gal staining in the forelimb bud (L) is restricted to cells of the dorsal and ventral premuscle masses (*27*). Cells of the presumptive diaphragm also expressed the *lac*Z transgene (arrow).

Four of fourteen embryos injected with F3′/−2.5lacZ contained *lac*Z-expressing cells. In all four embryos, this transgene was activated in cells from every skeletal muscle–forming region shown by in situ analyses (*8, 9*) to express the endogenous *myo*D gene. The most prominent feature of these embryos was the intense staining of the somites and limb buds. Somite staining yielded a metameric pattern of β-gal–positive cells along the central axis of the embryo (Fig. 4B). Observations of histological sections of three embryos demonstrated that somitic *lac*Z staining was confined to cells in the myotomal compartment of the somite (Fig. 4C). At 11.5 days p.c., *lac*Z-expressing cells were observed in the myotomes of only the 20 to 25 most rostral somites; *lac*Z expression was not detected in somites approximately at the level of, or caudal to, the hind limb (Fig. 4B). In later stage embryos all somites expressed the *lac*Z transgene (*24*). This clearly defined rostrocaudal gradient of *lac*Z expression, which corresponds to the gradient of transcript accumulation for *myo*D and the other myogenic regulatory factors (*8–10*), reflects the rostrocaudal sequence of somite formation and maturation (*25*). The lacZ transgene is likely activated in a ventral to dorsal sequence because *lac*Z-expressing cells are confined to the ventral myotome in less mature caudal somites, but are present throughout the ventral-dorsal myotomal axis in more mature anterior somites (Fig. 4B).

All four *lac*Z-positive embryos contained β-gal–expressing cells in the proximal region of both the fore- and hind-limb buds (Fig. 4B). These cells were localized to the dorsal and ventral premuscle masses (Fig. 4D), which give rise to the skeletal musculature of the limb. The forelimb contained large populations of cells that expressed the transgene, whereas the hind limb contained few *lac*Z-expressing cells (Fig. 4, B and D). Because myoblasts of the developing limb buds are derived from the somite dermomyotome (*26*), the smaller population of *lac*Z-expressing cells in the hind-limb bud probably reflects the earlier developmental stage of the somites at the level of the hind limb compared to rostral somites at the level of the forelimb.

The *lac*Z-expressing cells were also observed in the visceral arches, evident in

whole mounts as patches or anteroposterior arrays of stained cells (Fig. 4B). In histological sections, groups of stained cells were found in the mesenchyme of the visceral arches, organized in centrally and peripherally localized masses (*24*). Transcripts for MyoD, myogenin, and Myf-5 colocalize to these regions of the visceral arches (*9, 10, 24*), which is composed of cells that will contribute to pharyngeal and facial musculature. In addition, presumptive muscle of the developing diaphragm stains intensely for β-gal (Fig. 4D). The *lac*Z transgene was not expressed in smooth and cardiac muscle (Fig. 4B), muscle types that do not express *myo*D. A stable transgenic line carrying this *lac*Z transgene gave the same, skeletal muscle–specific pattern of *lac*Z expression (*24*).

Our transgenic data establish that the *myo*D enhancer and promoter are the DNA targets through which *myo*D expression is regulated. An apparent paradox exists between the lineage-specific regulation imposed on the enhancer-promoter transgene during early development and the lack of muscle-specific regulation of these control elements in cell culture. Transfection data demonstrate that many nonmyogenic cell lines contain positive trans-acting factors that can activate the *myo*D enhancer and promoter, yet the chromosomal *myo*D gene in these cells is repressed. We suggest that repression of the chromosomal *myo*D gene in these cells is a result of mechanisms that restrict accessibility of enhancer and promoter elements to trans regulators. A role for DNA methylation in cis repression has been indicated by the findings that 5-azacytidine converts 10T1/2 cells to the myogenic lineage (*1*) and activates the chromosomal *myo*D gene (*2*). Alternatively, cell hybrid experiments have suggested that *myo*D is repressed by negative trans-acting factors in primary human fibroblasts (*20*). In the embryo, *myo*D is likely regulated at multiple levels that may include derepression of both cis and trans negative control systems in the skeletal muscle lineage.

REFERENCES AND NOTES

1. S. F. Konieczny and C. P. Emerson, Jr., *Cell* **38**, 791 (1984).
2. R. L. Davis, H. Weintraub, A. B. Lassar, *ibid.* **51**, 987 (1987).
3. D. G. Edmondson and E. N. Olson, *Genes Dev.* **3**, 628 (1989); W. E. Wright, D. A. Sassoon, V. K. Lin, *Cell* **56**, 607 (1989).
4. T. Braun, G. Buschhausen-Denker, E. Bober, H. H. Arnold, *EMBO J.* **8**, 701 (1989).
5. S. J. Rhodes, and S. F. Konieczny, *Genes Dev.* **3**, 2050 (1989); T. Braun, E. Bober, B. Winter, N. Rosenthal, H. H. Arnold, *EMBO J.* **9**, 821 (1990); J. H. Miner and B. Wold, *Proc. Natl. Acad. Sci. U.S.A.* **87**, 1089 (1990).
6. H. Weintraub *et al.*, *Science* **251**, 761 (1991); E. N. Olson, *Genes Dev.* **4**, 1454 (1990); C. P. Emerson, Jr., *Curr. Opin. Cell Biol.* **2**, 1065 (1990).
7. C. Murre, P. S. McCaw, D. Baltimore, *Cell* **56**, 777 (1989).
8. D. Sassoon *et al.*, *Nature* **341**, 303 (1989).
9. M.-O. Ott, E. Bober, G. Lyons, H. Arnold, M. Buckingham, *Development* **111**, 1097 (1991).
10. E. Bober *et al.*, *J. Cell Biol.* **113**, 1255 (1991); T. J. Hinterberger, D. A. Sassoon, S. J. Rhodes, S. F. Konieczny, *Dev. Biol.* **147**, 144 (1991).
11. A full-length mouse MyoD cDNA (*18*) was used to screen a pWE15 human genomic Mbo I cosmid library (Stratagene, La Jolla, CA). Approximately 400,000 colonies on 20 duplicate nitrocellulose filters were hybridized (*28*) at moderate stringency (65°C for prehybridization and hybridization, 55°C for washes) with a ^{32}P-labeled random-primed mouse MyoD1 cDNA. Three overlapping clones were obtained that contained the entire *myo*D coding sequence with varying amounts of 5′ and 3′ sequence. Eco RI maps were generated by the indirect end-labeling method as described (*29*). All three cosmid clones were identical from the distal Not I site through the *myo*D gene. The approximate sizes of the restriction fragments of chMD-13 are as follows: 1, 1.7 kb; 2, 1.9 kb; 3, 4.1 kb; 4, 0.45 kb; 5, 9.7 kb; 6, 0.65 kb; 7, 0.25 kb; 8, 3.9 kb; 9, 6.4 kb; and 10, 2.8 kb.
12. T. Braun *et al.*, *EMBO J.* **8**, 3617 (1989).
13. ptkCATΔEH (derived from pBLCAT2 (*30*) by deletion of the Nde I–Hind III fragment of pUC18) was used in all transfection experiments. All cloning procedures were by standard methods. A 2.8-kb fragment containing the *myo*D promoter (derived from a pBluescript II KS+ sequencing deletion) was generated by digestion with Sac I followed by partial digestion with Kpn I (both sites derive from the multiple cloning site of pBluescript) and was blunt-end–ligated into ptkCATΔEH after digestion with Xba I and Bgl II [thereby removing all HSVtk promoter sequences (from −105 to +51)]. The resulting construct contains ~2.7 kb of human sequences extending from an Eco RI site ~2.5 kb 5′ of the *myo*D gene (see Fig. 1A) to +198 relative to the TATA box (nucleotide −37 relative to the start of translation). The −24CAT construct was generated by digesting chMD-13 with Not I, followed by partial cleavage with Eco RI. Partial cleavage products were size-fractionated on a 0.6% agarose gel, and fragments of about 20 to 25 kb were gel-purified and directionally cloned into −2.5CAT that had been digested with Not I and partially digested with Eco RI (vector sequences in −2.5CAT contain two Eco RI sites). The resulting clone contains contiguous human sequences from the distal Not I site through +198. Fragments 2 through 8 were cloned into the Xba I site of −2.5CAT by digesting chMD-13 with Not I and Eco RI, and blunt-end–ligating fragments into the unique Xba I site (see Fig. 1A). Fragment 3 was cloned in both orientations upstream of the tk promoter by blunt-end ligation into the unique Bam HI site (F3/tkCAT and F3′/tkCAT). The −24ΔF3CAT construct was generated by partially digesting −24CAT with Eco RI, ligating gel-purified, size-selecting digestion products, and screening by colony hybridization for clones missing only fragment 3.
14. All cell lines were obtained from the American Type Culture Collection except 23A2, which was derived from 10T1/2 cells by 5-azacytidine treatment (*1*). C3H10T1/2 and 23A2 cells were maintained in basal medium Eagle's (BME) medium supplemented with 15% fetal bovine serum (FBS). JEG-3 human choriocarcinoma cells were maintained in Dulbecco's modified Eagle's medium (DMEM) supplemented with 10% FBS. HepG2 human hepatoma cells were maintained in 50:50 DMEM:Ham's F12 supplemented with 10% FBS. All media was supplemented with penicillin G (100 U/ml) and streptomycin sulfate (100 μg/ml) (Gibco, Grand Island, NY). All DNAs used in transfections were prepared by alkaline lysis and double-banded in CsCl gradients. Cells were transfected by the calcium phosphate precipitation method as follows. Cells were trypsinized and plated at 2×10^5 cells per 100-mm plate (10T1/2 and 23A2 cells) or passed ~1:10 from 50% confluent plates (JEG-3 and HepG2 cells). The following day cells were fed fresh medium, and 3 hours later calcium phosphate–DNA coprecipitates (1 ml per 100-mm dish) were added (0.8 pmol of test plasmid, brought to 25 μg with plasmid carrier DNA). About 16 to 18 hours later, the precipitates were removed, cells washed one time in basal medium without FBS, and then fed complete medium. After 48 hours, cells were harvested and lysed by freeze-thawing (*31*). CAT enzyme activity in cell extracts was quantified with the xylene extraction method (*32*) with ^{3}H-labeled chloramphenicol (31.2 Ci/mmol; New England Nuclear) and N-butyryl coenzyme A (Sigma, St. Louis, MO). Equivalent amounts of protein (15 to 25 μg as determined with a Bio-Rad protein kit and bovine serum albumin as a standard) and a reaction time of 1 hour was used in all CAT assays, which kept all values within the linear range of the assay. In a typical experiment with 15 μg of protein, 1% conversion of ^{3}H-labeled chloramphenicol to butyryl ^{3}H-chloramphenicol was ~45,000 cpm as determined by scintillation counting.
15. D. J. Goldhamer and C. P. Emerson, Jr., unpublished data.
16. T. B. Vaidya, S. J. Rhodes, E. J. Taparowsky, S. F. Konieczny, *Mol. Cell. Biol.* **9**, 3576 (1989).
17. In some experiments, −24ΔF3CAT yielded CAT activities approximately twofold higher than −2.5CAT. This is likely a result of low activity of fragment 5; F5/−2.5CAT also yielded CAT activities approximately twofold higher than −2.5CAT (Fig. 1B).
18. D. F. Pinney, S. H. Pearson-White, S. F. Konieczny, K. E. Latham, C. P. Emerson, Jr., *Cell* **53**, 781 (1988).
19. A. Salminen *et al.*, *J. Cell Biol.* **115**, 905 (1991).
20. M. J. Thayer and H. Weintraub, *Cell* **63**, 23 (1990).
21. M. J. Thayer *et al.*, *ibid.* **58**, 241 (1989).
22. The *lac*Z vector pPD46.21 was used in transgene constructions. pPD46.21 is identical to pPD1.27 (*33*) except that it lacks the *sup-7* gene. It contains an initiation codon and SV40 T antigen nuclear localization signal just upstream from *lac*Z, and polyadenylation sequences from the SV40 early region downstream of *lac*Z (*33*). The −2.5lacZ and F3′/−2.5lacZ vectors were constructed by digesting −2.5CAT and F3′/−2.5CAT at flanking Sal I and Xho I sites (Fig. 1A), and cloning gel-purified fragments into the Sal I site in the 5′ polylinker of pPD46.21 (thereby destroying the Xho I site). The −2.5lacZ and F3′/−2.5lacZ vectors yielded a faint or intense, nuclear localized signal, respectively, after transient transfection into 23A2 myoblasts (*15*). DNAs for injections were digested with Not I to remove pUC19 sequences, and *lac*Z fusions were purified on agarose gels. Microinjections of the plasmid-free *lac*Z fusion genes into the pronuclei of fertilized eggs of the inbred strain FBV/N were performed [as described (*34*)]. Embryos 11.5 days p.c. were stained for β-gal as follows. Embryos were fixed for 30 to 60 min in 1% paraformaldehyde, 0.2% glutaraldehyde in 0.1 M phosphate buffer, pH 7.4. After rinsing, embryos were stained for β-gal as described (*35*). Following photomicrography, the embryos were embedded in paraffin, serially sectioned at 8 μm, and sections were counterstained with nuclear fast red.
23. N. D. Allen *et al.*, *Nature* **333**, 852 (1988); R. D. Palmiter and R. L. Brinster, *Annu. Rev. Genet.* **20**, 465 (1986).
24. A. Faerman and M. Shani, unpublished data.
25. R. Rugh, *The Mouse: Its Reproduction and Development* (Oxford Univ. Press, Oxford, 1990).
26. A. Chevallier, M. Kieny, A. Mauger, *J. Embryol. Exp. Morphol.* **41**, 245 (1977); B. Christ, H. J. Jacob, M. Jacob, *Anat. Embryol.* **150**, 171 (1977).
27. At 11.5 days p.c. the limb is surrounded by a single cellular layer of undifferentiated epithelium. The *lac*Z staining near the periphery of the limb bud is in myogenic cells, not cells of the skin, which does not begin to differentiate until 14 days p.c. (*25*).
28. K. Peden, P. Mounts, G. S. Hayward, *Cell* **31**, 71 (1982).
29. G. M. Wahl *et al.*, *Proc. Natl. Acad. Sci. U.S.A.* **84**, 2160 (1987).

30. B. Luckow and G. Schutz, *Nucleic Acid Res.* 15, 5490 (1987).
31. F. Ausubel *et al.* (Eds.) *Current Protocols in Molecular Biology* (Wiley, New York, 1989), vols. 1 and 2.
32. B. Seed and J.-Y. Sheen, *Gene* 67, 271 (1988).
33. A. Fire, S. White-Harrison, D. Dixon, *ibid.* 93, 189 (1990).
34. B. Hogan, F. Costantini, E. Lacy, *Manipulating the Mouse Embryo: A Laboratory Manual* (Cold Spring Harbor Laboratory, Cold Spring Harbor, NY, 1986); M. Shani *Mol. Cell. Biol.* 6, 2624 (1986).
35. J. R. Sanes, J. L. R. Rubinstein, J. F. Nicolas, *EMBO J.* 5, 3133 (1986).
36. We thank I. Akerblom, B. Brunk, J. Burch, R. Perry, D. Pinney, and B. Pownall for critical comments on the manuscript and for helpful discussions. We thank A. Fire and J. Altschmeid for providing pPD46.21 and ptkCATΔEH, respectively. D.J.G. was supported by a Jere Thompson Neuromuscular Research Fellowship from the Muscular Dystrophy Association. Supported by a CORE grant (CA-06927) from NIH and an appropriation from the Commonwealth of Pennsylvania; by research grants from the Muscular Dystrophy Association and the National Institutes of Child Health and Human Development (HD-07796) to C.P.E.; by the United States–Israel Binational Agricultural Research and Development Fund to C.P.E. and M.S.; and by grants from the Israel Academy of Science and Humanities and the Ministry of Sciences and Development to M.S. We also thank the University of Virginia, where these studies were initiated.

9 December 1991; accepted 26 February 1992

Participation of Tyrosine Phosphorylation in the Cytopathic Effect of Human Immunodeficiency Virus–1

David I. Cohen,* Yoshihiko Tani, Huan Tian, Elizabeth Boone, Lawrence E. Samelson, H. Clifford Lane

Protein tyrosine phosphorylation is a common mechanism of signaling in pathways that regulate T cell receptor–mediated cell activation, cell proliferation, and the cell cycle. Because human immunodeficiency virus (HIV) is thought to affect normal cell signaling, tyrosine phosphorylation may be associated with HIV cytopathicity. In both HIV-infected cells and transfected cells that stably express HIV envelope glycoproteins undergoing HIVgp41-induced cell fusion, a 30-kilodalton protein was phosphorylated on tyrosine with kinetics similar to those of syncytium formation and cell death. When tyrosine phosphorylation was inhibited by the protein tyrosine kinase inhibitor herbimycin A, envelope-mediated syncytium formation was coordinately reduced. These studies show that specific intracellular signals, which apparently participate in cytopathicity, are generated by HIV and suggest strategies by which the fusion process might be interrupted.

Despite intensive scrutiny, the mechanisms by which HIV infection depletes antigen-specific $CD4^+$ helper T cells and leads to the development of acquired immunodeficiency syndrome (AIDS) are incompletely understood (*1*). Immunodeficiency caused by HIV infection is likely to result from direct T cell killing (*2*) and the disruption of T cell function by the virus (*3*). Interference by HIV with antigen-specific helper cell triggering has been extensively documented in in vitro studies (*4*).

Tyrosine phosphorylation participates directly in the regulation of cell growth, in T cell receptor (TCR)–and CD4 receptor–mediated signaling, and in antigen-specific T cell proliferation. Normal antigen-specific triggering of helper T cells leads to the rapid tyrosine phosphorylation of the TCR ζ chain and other cellular substrates (*5*), and inhibition of tyrosine phosphorylation suppresses TCR-mediated cell proliferation (*6, 7*). Several enzymes controlling the cell cycle are regulated by tyrosine phosphorylation, and aberrant expression of certain kinases associated with cell cycle control, such as $p107^{wee1}$, also may lead to abnormal cell morphology (*8*). The kinase $p107^{wee1}$ contributes to the inhibitory tyrosine phosphorylation of the $p34^{cdc2}$ cell cycle kinase (*9–12*). Tyrosine dephosphorylation of $p34^{cdc2}$ is required for the G_2 to M phase transition in normal cell division.

We investigated the effects of HIV on T cell signal transduction pathways by examining the phosphotyrosine content of intracellular proteins. In response to infection of T cells with HIV-1 LAV, the amount of tyrosine phosphorylation of 30-, 40-, and 95-kD substrates increased in both Jurkat cells or in peripheral blood lymphocytes (PBLs) as compared to uninfected Jurkat cells or uninfected PBLs (Fig. 1) (*13*). Proteins of 40- and 95-kD become tyrosine-phosphorylated after cross-linking of CD3-TCR, but not CD4 or CD45 receptors in Jurkat cells or PBLs (*6, 7*). There have been no reports of a 30-kD substrate undergoing tyrosine phosphorylation in response to T cell activation (*6, 7*).

All of the substrates displayed their highest levels of tyrosine phosphorylation during the fourth day of infection (*14*), ranging from 5.0 to 8.0 times the initial levels for the 135-, 95-, and 40-kD proteins (Fig. 2A). No phosphorylation of the TCR ζ chain was observed. The increase in tyrosine phosphorylation of the 30-kD substrate (pp30) was the largest (23-fold) and slightly more persistent. Tyrosine phosphorylation of pp30 occurred early in the course of HIV infection compared to the production of viral proteins or the activity of reverse transcriptase (RT) in the medium, both of which were maximal after 5 days of culture (Fig. 2B).

To confirm that pp30 from HIV-infected cultures contained phosphotyrosine, we subjected pp30 to phosphoamino acid analysis. Jurkat cells were labeled with ^{32}P-orthophosphate 5 days after infection with HIV-1. The pp30 protein contained phosphotyrosine, phosphothreonine, and phosphoserine (Fig. 3) (*15*). This pattern of phosphorylation on tyrosine and threonine residues has been reported for at least one cell cycle kinase, $p34^{cdc2}$ (*9, 11, 16*).

The interaction of the HIV-envelope glycoproteins, which mediate CD4 binding (*17*), with the T cell signal transduction apparatus could potentially generate signaling abnormalities or lethal events. To study this possibility, we selected transfected Jurkat T cells that stably expressed HIV-envelope glycoproteins (*18*). We used an envelope-transfected cell line, HIV-env (2-8),

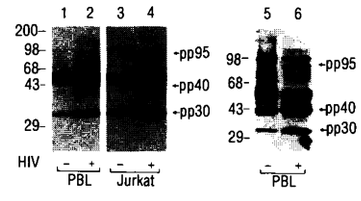

Fig. 1. Induction of tyrosine phosphorylation after infection of cells with HIV-1 LAV. Protein lysates from 5×10^6 peripheral blood lymphocytes (PBLs) (lanes 1, 2, 5, and 6) or Jurkat cells (lanes 3 and 4) either incubated with medium alone (−) or infected with medium containing HIV-1 LAV (+) were resolved on SDS-polyacrylamide gradient gels (10 to 20%), transferred for protein immunoblot analysis, probed with rabbit polyclonal antibody to phosphotyrosine, and developed with ^{125}I-labeled protein A (*13*). Size markers are indicated to the left of the gels (in kilodaltons); proteins with prominently augmented tyrosine phosphorylation (pp) are indicated by their molecular size (in kilodaltons) to the right.

D. I. Cohen, Y. Tani, H. Tian, E. Boone, H. C. Lane, Laboratory of Immunoregulation, National Institute of Allergy and Infectious Diseases, National Institutes of Health, Bethesda, MD 20892.
L. E. Samelson, Cell Biology and Metabolism Branch, National Institute of Child Health and Development, National Institutes of Health, Bethesda, MD 20892.
*To whom correspondence should be addressed.